9A.2 APPLICATION OF ANISOTROPIC RECURSIVE FILTERS TO THE GENERATION OF PLANETARY SCALE BACKGROUND COVARIANCES

Yoshiaki Sato,
On leave from Japan Meteorological Agency, visiting NOAA/NCEP/EMC, Camp Springs, MD
R. James Purser*
Science Applications International Corporation, NOAA/NCEP/EMC, Camp Springs, MD

1. INTRODUCTION

NCEP's Spectral Statistical Interpolation (SSI, see Parrish and Derber 1992) has recently been replaced by a grid-point statistical interpolation (GSI, see Wu et al. 2002, Kleist et al. 2009) The global synthesis of background error covariances in the GSI is presently done by performing recursive filtering operations (Purser et al. 2003a,b) on three overlapping domains and merging the results. The domains are:

- a southern polar stereographic domain with Cartesian grid coordinates;
- a central domain with cylindrical grid coordinates;
- a northern polar stereographic domain similar to its southern counterpart.

The purpose of dividing the region in this way is to ensure that the numerical operations of recursive filters do not encounter coordinate singularities.

The covariances may be generated on each of the overlapping grids and the results smoothly blended. However, in the stratosphere and mesosphere, the horizontal scales of the covariances may be very large; in this case it is found that width of the grid overlap is insufficient to prevent a slight distortion of the final covariances within the blending zones.

In the next section we propose a remedy based on a very different kind of global gridding which exploits the full three-dimensional nature of the geometry, but abandons the usual convention by which one 'vertical' coordinate adheres to approximately horizontal surfaces.

2. CUBIC GRIDDING

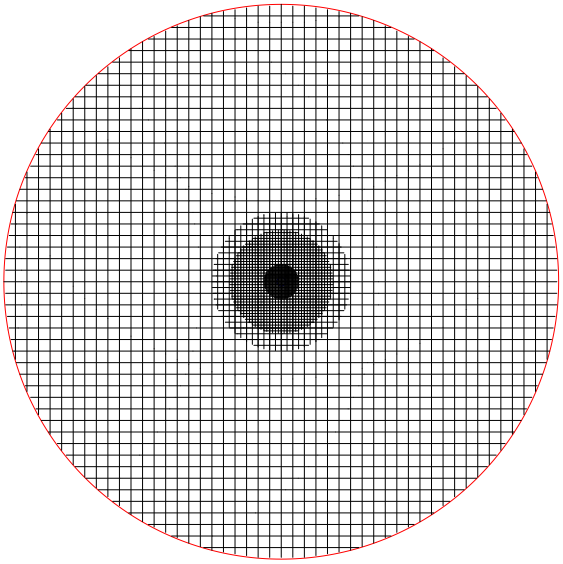

Figure 1: Nested Cartesian grids, of unequal spans

Instead of separating the quasi-horizontal levels by one 'vertical' coordinate and expecting two other 'horizontal' coordinates to cover the spherical surface, we transform the three-dimensional spherical shell occupied by the atmosphere to the interior of an abstract cube which can then be gridded in Cartesian fashion to avoid any coordinate singularity whatsoever. This somewhat radical solution, while woefully inadequate as a strategy for modeling, is perfectly satisfactory as a means for supplying a grid on which anisotropic filtering can proceed unmolested by singularities (which pose a greater threat than does the lack of stratification). Obviously, embedding the atmosphere directly and without metrical distortion is impractical since the

*Corresponding author address: R. J. Purser, W/NP2 RM 207, WWBG, 5200 Auth Road, Camp Springs, MD 20746

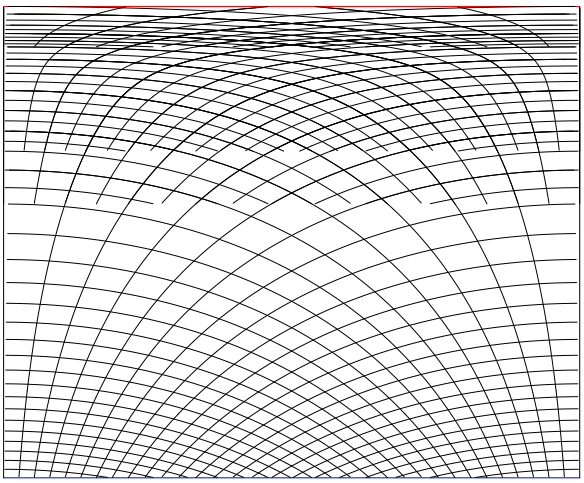

Figure 2: A non-logarithmic radial transformation of the nested Cartesian grids of Fig. 1, showing a vertically nonuniform resolution in both the vertical and horizontal directions. The horizontal extent of the nested configuration of grids sketched here is one quadrant of the Earth; the vertical scaling is linear in the pseudo-height, $\log(\sigma)$.

atmosphere's effective thickness is tiny (a few tens of kilometers) compared to Earth's radius (a few thousand kilometers). On the other hand, if we radially transform the thin atmospheric shell to a very much thicker one, comparable to the Earth's radius, we make fuller use of the cubic grid.

However, if transforming to a very thick image shell, the lower atmosphere will be resolved relatively poorly (in the horizontal direction) compared to the upper atmosphere. It would be preferable to confer on the upper portion of the atmosphere the lower resolution in the horizontal directions, which suggests that 'inverting' the radial ordering in the transformation would be a better arrangement.

Another way of exerting control over the resolution is to refine the inner portion of the cubic grid where the resolution is otherwise deficient and, if necessary, to repeat such refinements in 'telescoping' fashion to create a hierarchic series of successively refined grids nested, each one within its predecessor, like Russian matryoshka dolls.

Trimming the corners, we might then have a cubic grid configuration analogous to the two-dimensional square grid depiction given in Fig. 1. Note that the 'span' of the grid (the number of its grid spaces across its width) need not be the same for each nest. Also, we need not choose simply the logarirthmic radial transformation to obtain the $\log(\sigma)$ quasi-height in the atmospheric model (which would lead to approximately uniform vertical resolution across the succession of nests) but, instead, we may smoothly vary the radial transformation away from this ideal, in order to enhance or degrade vertical resolution in a controlled way at each altitude. The details of how this might be done are described in Sato and Purser (2009).

A two-dimensional example of the transformation of the nested grids corresponding to the configuration of Fig. 1, is shown in Fig. 2, where a radial transformation has been chosen to enhance the vertical resolution at the top, where the span of the finest nesting also gives only relatively poor horizontal resolution. Each grid can support a filtering operation with a characteristic scale suitable to that grid and, provided an amplitude-modulating function causes the amplitude of each grid's filter to drop smoothly to zero at or before the grid's boundary, the contributions of all the nested grids can be added up when interpolated back to the principal overlapping analysis grids used to cover the globe.

3. TESTING THE NESTED GRIDS IN THE GSI

The approximately ellipsoidal shape of the background error covariance of a control variable at any geographical location and altitude can now be transformed to the corresponding ellipsoidal shape parameters ('aspect tensor components') within the nested cubic grids. The ability to construct anisotropic quasi-diffusive smoothing filters by applying the 'Hexad algorithm' with recursive filters (Purser et al. 2003b) to reproduce covariances of any ellipsoidal shape, regardless of their oblique orientations relative to the grid, makes the covariance in the nested grid domains as easy to work with as it is in the standard three-patch overlapping grids. But for covariance contributions that have very large horizontal scales the advantage is that no horizontal overlap intrudes to distort the shapes of these covariance contributions.

The present operational GSI employs the simpler, horizontally isotropic, form of the recursive filtering package to generate its quasi-Gaussian covariance contributions, but the adaptive anisotropic covariance operators are available for experiments. In Fig. 3 the panels on the extreme left show covariances produced by the operational isotropic method, while the central panels show the corresponding results formed by the more general anisotropic algorithm, still within the same three-patch grid configuration, but with parameters set to mimic the

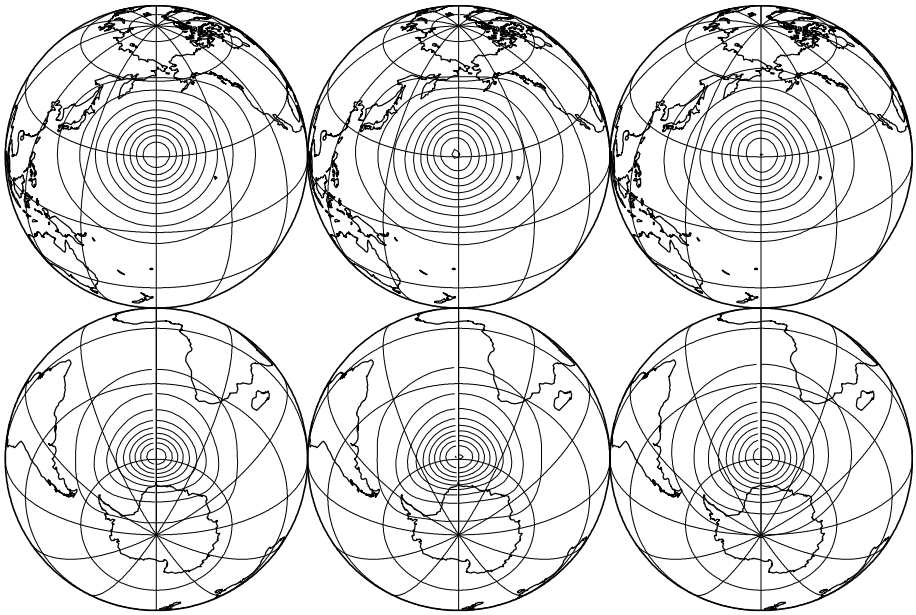

Figure 3: Covariance construction test result at $\log_2(\sigma) = -6.24$ (13.4mb) with the contour interval of 0.1. The initial signals are put at (180°E, 30°N) (upper panels) and at (0°E, 60°S) (lower panels). The left column shows the standard GSI (isotropic mode) result, the center column shows the anisotropic mode GSI result, and the right column shows the anisotropic mode GSI with cubic grid results.

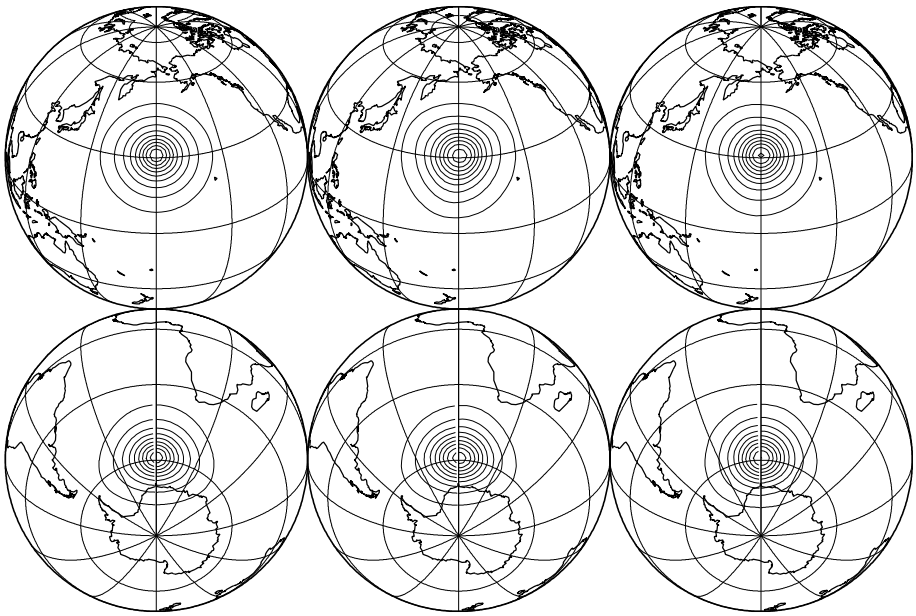

Figure 4: Same as Fig. 3 but at $\log_2(\sigma) = -2.23$ (216mb).

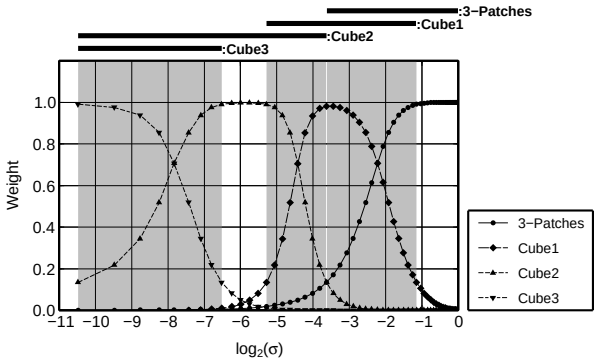

Figure 5: Weighting functions for the each cubic grid space and original three patch system. The square-sum of the weighting function is one.

isotropic results. The impulses forcing these responses lie at 13.4mb and at (180°E, 30°N) in the upper panels, at (0°E, 60°S) in the lower panels. The right panels show the production of the same covariance samples using the three-dimensionally nested grids and, of course, the fully anisotropic filters. The respective covariances generated within the three-patch configuration by the isotropic and anisotropic filter algorithms for at each sample location are virtually identical, confirming that the alternative filter algorithm behaves consistently. However, in each case, we see evidence of the artificial anisotropy resulting from the presence of the mid-latitude blending zones. This anisotropy is not present in the right panels, showing that the nested grids method successfully resolves this defect.

Some subtle residual unevenness in the contours for the cases involving the anisotropic filters is probably the consequence of sampling variations in the stochastic method presently used to renormalize these covariances; this effect is expected to be eliminated by the new normalization method based on the asymptotic 'Parametrix Expansion' method described by Purser (2008a,b).

Fig. 4 shows the covariance contributions generated at the same geographical locations, but at a lower altitude (216mb) where the covariance scales are much smaller. In these cases, the adverse effects of the overlapping grids are less visible in the left and central panels, as we would expect, since these covariances fit more comfortably within the blending zones where the grids overlap.

The configuration of cubes, and the weights attributed to their contributions to the covariance synthesis, and the weight attributed to the three-patch combination, are all shown in Fig. 5. At the altitude (216mb) of the impulses used in Fig. 4, with $\log_2(\sigma) = -2.23$, a significant contribution to the covariances of the two right panels still comes from the three-patch conventional grids, so these covariances are still slightly affected by the presence of the blending zones. But at the higher altitude of Fig. 3, the entire synthesis of the covariances shown in the two right panels comes from the nested cubes.

4. NON-CARTESIAN GRIDDING

The nested grid experiments were carried out using a simple regular Cartesian lattice for each cube and the wasted space *not* occupied by its embedded sphere occupies almost the same amount of volume as the sphere itself. But the fact that covariance generation in these domains *must* be conducted using the more general anisotropic filters has the liberating consequence that it is no longer necessary to restrict the computational lattice here to be of the simple 'cubic' variety as regarded in Earth-centered Cartesians. Other simple lattices, familiar in crystallography, resolve space more isotropically. One of these, the 'face centered cubic' (fcc) lattice (e.g., Ziman 1979) is associated with the closest regular packing arrangement of identical spheres. As a consequence of this property, the embedded spherical region of concern to this grid nest also occupies the largest possible proportion (about 74%) of the volume of the most accommodating 'fundamental polyhedron' of any periodic extension of each lattice-and-sphere combination.

The fundamental polyhedron in which the sphere can be inscribed most efficiently is the Voronoi cell of the fcc lattice (a Voronoi cell comprises all the points closer to a selected lattice point than to any other lattice point).

The generating vectors of the fcc lattice, relative to the Cartesian coordinates, are proportional to the columns of the matrix,

$$E = \begin{bmatrix} 0, & 1, & 1 \\ 1, & 0, & 1 \\ 1, & 1, & 0 \end{bmatrix}$$

and the Voronoi cells of such a lattice can be shown to have the shape of the 'rhombic dodecahedron' (e.g., Coxeter, 1963). But a linear transformation by a matrix proportional to

$$2E^{-1} = \begin{bmatrix} -1, & 1, & 1 \\ 1, & -1, & 1 \\ 1, & 1, & -1 \end{bmatrix}$$

transforms the fcc grid into a cubic one, the sphere into an oblate ellipsoid; a triply-periodic cubic domain in this *transformed space*, just large enough to

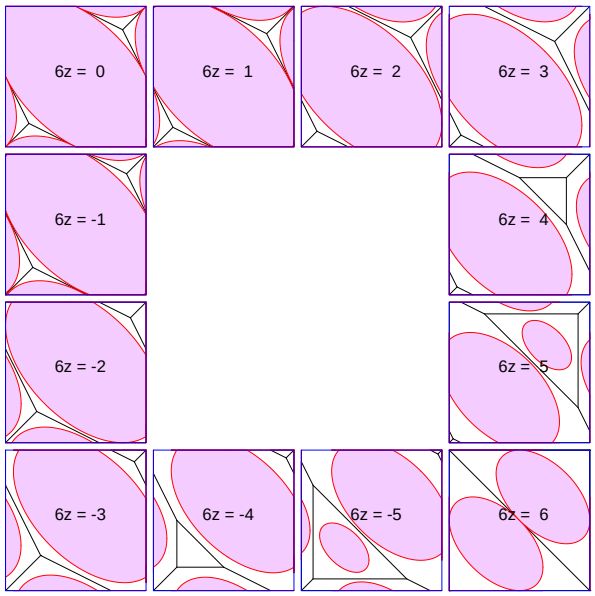

Figure 6: Schematic depiction of the efficient non-overlapping embedding of a spherical volume (shaded, shown in a cyclic succession of constant-z cross-sections) in a periodic cubic 'x, y, z' grid via a linear distortion that would convert the locally cubic lattice into one metrically equivalent to the more isotropic face-centered cubic lattice. Polygonal segments within each square section show the Voronoi cell boundary, similarly distorted.

accommodate the ellipsoid without overlap, consequently improves simultaneously the isotropy (in the original Cartesian space) of grid resolution, and the efficiency of utilization of the computational array. Fig. 6 vividly demonstrates, through one cycle of cross-sections through the logically-cubic periodic array, that the domain of interest (shaded ellipsoid) packs very efficiently, and without overlap, into the space available for it. This rather simple geometrical device will be considered for future implementations of the nested grid method.

5. DISCUSSION

We have proposed, and successfully tested, a way of overcoming a minor defect of the present GSI as it affects the very largest horizontal scales of covariances. Our method employs a nested sequence of cubic grids constructed to resolve these large scales in the upper levels of the domain of the global analysis. Preliminary experiments with cycled assimilation at T62 resolution have shown a mixture of positive and negative impacts. The worst negative impacts involved the very top levels of the model where our interpolation procedures are known to be deficient. The ability to accommodate horizontally anisotropic, and arbitrarily tilted, covariances within the new system has not been exercised in the experiments conducted so far. Neither have we fully exploited the inherent 'multigrid' aspect of the nested grid configuration, which, without additional significant cost, could allow us in future to reshape the covariances to exhibit more general profiles than the simple quasi-Gaussian shapes we have confined our studies to.

Replacing the present cubic grids with the alternative oblique grid nests using the face-centered cubic lattice discussed in Section 4 may improve the computational efficiency significantly. Also, should the general method be adopted, it might enable the horizontal extent of the present blending zones of the three-patch configuration, used in this future context only for the very finest scales of covariance contributions, to be dramatically reduced, entailing a concomitant computational saving through the reduction in the amount of storage, filtering, interpolation and blending needed to generate and reconcile the partial solutions allocated to these three patches. At higher altitudes, where the covariance's horizontal scales are very large, it might not even be necessary to perform *any* recursive filtering on the three-patch grids, further reclaiming the computational costs (an increase of about 34% in our preliminary experiments) incurred by the introduction of these new supplementary nested grids into the analysis configuration.

ACKNOWLEDGMENTS

The authors would like to thank Drs. Manuel Pondeca, David Parrish, Wan-Shu Wu, John Derber and Henry Juang for the helpful discussions and suggestions. This work was carried out under the collaboration of NCEP and JMA, supported by UCAR. The authors also would like to thank those concerned with this program.

REFERENCES

Coxeter, H. S. M., 1963: *Regular Polytopes*, Dover, New York. 321 pp.

Kleist, D. T., D. F. Parrish, J. C. Derber, R. Treadon, R. M. Errico, and R. Yang, 2009: Improving incremental balance in the GSI 3DVAR analysis system. *Mon. Wea. Rev.,* **137,** 1046–1060.

Parrish, D. F., and J. C. Derber, 1992: The National Meteorological Center's Spectral Statistical-Interpolation Analysis System. *Mon. Wea. Rev.,* **120,** 1747–1763.

Purser, R. J., 2008a: Normalization of the diffusive filters that represent the inhomogeneous covariance operators of variational assimilation, using asymptotic expansions and techniques of non-Euclidean geometry; Part I: Analytic solutions for symmetrical configurations and the validation of practical algorithms. NOAA/NCEP Office Note 456, 48 pp.

Purser, R. J., 2008b: Normalization of the diffusive filters that represent the inhomogeneous covariance operators of variational assimilation, using asymptotic expansions and techniques of non-Euclidean geometry; Part II: Riemannian geometry and the generic parametrix expansion method. NOAA/NCEP Office Note 457, 55 pp.

Purser, R. J., W. Wu, D. F. Parrish, and N. M. Roberts, 2003a: Numerical aspects of the application of recursive filters to variational statistical analysis. Part I: spatially homogeneous and isotropic Gaussian covariances. *Mon. Wea. Rev.*, **131**, 1524-1535.

Purser, R. J., W. Wu, D. F. Parrish, and N. M. Roberts, 2003b: Numerical aspects of the application of recursive filters to variational statistical analysis. Part II: spatially inhomogeneous and anisotropic Gaussian covariances. *Mon. Wea. Rev.*, **131**, 1536-1548.

Sato, Y., and R. J. Purser, 2009: Singularity-free global telescoping grids suitable for large-scale global covariance synthesis by anisotropic recursive filtering. NOAA/NCEP Office Note 458.

Wu, W., R. J. Purser, and D. F. Parrish, 2002: Three dimensional variational analysis with spatially inhomogeneous covariances. *Mon. Wea. Rev.*, **130**, 2905-2916.

Ziman, J. M. 1979 *Principles of the Theory of Solids* Cambridge, 448 pp.